Supporting information

Ultrathin core-shell-satellite structured Au@PtPd@Pt nanowires for superior electrocatalytic hydrogen evolution†

Caikang Wang,‡[ac] Xian Jiang‡[a], Qicheng Liu,[d] Jiaqian Ding,[d] Juan Zhou,*[c] Yawen Tang,[d] Gengtao Fu[d] and Jong-Min Lee*[b]*

[a] School of New Energy, Nanjing University of Science and Technology, Jiangyin, 214443, China.

[b] School of Chemical and Biomedical Engineering, Nanyang Technology University, Singapore 637459, Singapore.

[c] School of Energy and Power Engineering, Nanjing University of Science and Technology, 200 Xiaolingwei Street, Jiangsu Province, 210094, China.

[d] Jiangsu Key Laboratory of New Power Batteries, Jiangsu Collaborative Innovation Centre of Biomedical Functional Materials, School of Chemistry and Materials Science, Nanjing Normal University, Nanjing 210023, China.

Corresponding Author

E-mail address: xianjiang@njust.edu.cn (X. Jiang); gengtaofu@gmail.com (G. Fu); jmlee@ntu.edu.sg (J.-M. Lee)

‡ These authors contributed equally to the paper.

Part I: Experimental

Chemicals and Reagents: 1-naphthol ($C_{10}H_8O$) was purchased from Aladdin (Shanghai, China). Hydrogen tetrachlorocuprate tetrahydrate ($HAuCl_4 \cdot 4H_2O$) and palladium chloride ($PdCl_2$) was supplied by Shanghai D&B Biological Science and Technology Co., Ltd. Chloroplatinic acid (H_2PtCl_6), polyvinylpyrrolidone (PVP), L-ascorbic acid (AA), sodium hydroxide (KOH) and ethanol (C_2H_5OH) were purchased from Sinopharm Chemical Reagent Co. Ltd (Shanghai, China). Nafion (5 wt.%) was purchased from Sigma-Aldrich Chemical Reagent Co., Ltd. Commercial 20% Pt/C was acquired from Johnson Matthey Corporation. Deionized water (DI water, 18.2 $M\Omega\ cm^{-1}$) was employed throughout all experiments. All chemicals were of analytical reagent grade and used without further purification.

Preparation of Au nanowires (NWs): The ultrathin Au NWs were prepared according to our previous work.[1] In a typical synthesis, 3.0 mL of 0.5 M 1-naphthol ethanol solution was added into 3.0 mL of 0.05 M $HAuCl_4$ aqueous solution at 60 °C under water bath conditions. After aging for a few minutes (~ 2 min), the resultant product was collected by centrifugation of 9000 rpm for 3 min, washed with ethanol several times, and re-dispersed in ethanol.

Preparation of Au@PtPd@Pt NWs: For the synthesis of Au@PtPd@Pt NWs, the well-dispersed Au NWs (6.0 mg) and 30 mg PVP were added into the mixed solution of 7.5 mL H_2O and 7.5 mL C_2H_5OH in a 30 mL vial. After uniform dispersion by sonication, 0.20 mL 0.05 M $PdCl_2$ and 0.20 mL 0.05 M H_2PtCl_6 aqueous solution were dissolved in the vial under vigorous stirring. Subsequently, 1.0 mL 0.10 M AA aqueous solution was immediately added to the resulting solution, and the vial was then immersed in a water bath held at 60 °C for 2h under magnetic stirring. After the reaction system cooled down to room temperature, the produced Au@PtPd@Pt NWs were finally collected by centrifugation 10000 rpm for 10 min and washed with ethanol six times.

Preparation of Au@Pt NWs and Au@Pd NWs: The synthesis of Au@Pt and Au@Pd NWs were similar to that of Au@PtPd@Pt NWs, except for substituting 0.20 mL 0.05 M H_2PtCl_6 + 0.20 mL 0.05 M $PdCl_2$ aqueous solution for 0.40 mL 0.05 M H_2PtCl_6 aqueous solution or 0.40 mL 0.05 M $PdCl_2$ aqueous solution, respectively.

Characterizations: Transmission electron microscopy (TEM), high-resolution TEM (HRTEM), high-angle annular dark-field scanning transmission electron microscopy (HAADF-STEM), and energy dispersive X-ray (EDX) elemental mapping measurements were made on a JEOL JEM-2100F transmission electron microscopy operated at an accelerating voltage of 200 kV. The crystallinity of the samples was determined by recording X-ray diffraction (XRD) patterns on a Model D/max-rC X-ray diffractometer using Cu Kα radiation source (λ = 1.5406 Å) and operating at 40 kV and 100 mA. X-ray photoelectron spectroscopy (XPS) measurements were performed with a Thermo VG Scientific ESCALAB 250 spectrometer with a monochromatic Al Kα X-ray source. The binding energy was calibrated by means of the C1s peak energy of 284.6 eV.

Electrochemical measurements: All electrochemical measurements were performed in a standard three-electrode electrochemical cell at ambient temperture using a CHI 760E workstation (CH Instruments, Shanghai, Chenhua Co., Ltd.). A graphite rod serves as auxiliary electrode and a saturated calomel electrode (SCE) works as reference electrode. For the preparation of catalyst inks, 2.0 mg prepared NWs or commercial Pt black and 2.0 mg Vulcan XC-72 carbon were well dispersed in 1.0 mL mixed solvent consisting of 0.60 mL ethanol and 0.30 mL H_2O, and 0.10 mL Nafion solution (5 wt.%) with the following sufficient sonication. Then, the glassy carbon electrode (d=3 mm) loaded with 10 μL of the mixed catalyst ink was used as the working electrode. Electrochemical HER was investigated in N_2-saturated 1M KOH solution with a sweeping rate of 5 mV s^{-1}. HER polarization curves were obtained using LSV with 95% *iR* compensation (*iR*, automatically measured with the CHI 760E electrochemical workstation). All electrode potentials were quoted versus reversible hydrogen electrodes (RHE). We conducted the RHE calibration with

reference to a method in the literature, while in our electrochemical test system of 1.0 M KOH, E(RHE) = E(SCE) + 1.071 V.[2] Turnover frequency (TOF) was calculated with using following equation: $TOF = jA/nFN$, where j is the current density under overpotential η = 50 mV, A is the geometric area of the working electrode, n is the electron transferred number in the HER reaction ion (*i.e.* 2), F is the Faraday constant of 96485.3 C mol^{-1}, and N is the number of active sites (mol) calculated with the total mass loading. Electrochemical double-layer capacitance (C_{dl}) was calculated from the CV curves tested in a non-Faradic region under different scan rates from 40 to 160 mV s^{-1}. The ECSA of the catalyst was estimated to be C_{dl}/C_s, where C_s respresents the specific capacitance of catalyst (0.06 mF cm^{-2}). To calculate j_{ECSA} of the catalysts, we normalized the measured current by the ECSA from the quation: $j_{ECSA} = i/ECSA$, where i is the measured current (mA), and ECSA is the ECSA value (cm^2). Electrochemical impedance spectroscopy (EIS) was tested over a frequency range of 100 kHz-0.1 Hz. The accelerated durability test (ADT) of CVs is performed between the potential range from -0.05 V to 0.05 V vs. RHE for 10,000 cycles with a scan rate of 100 mV s^{-1}. The long-term durability was recorded by chronopotentiometry measurement at 10 mA cm^{-2} for 27 h.

Part II: Figures and Tables

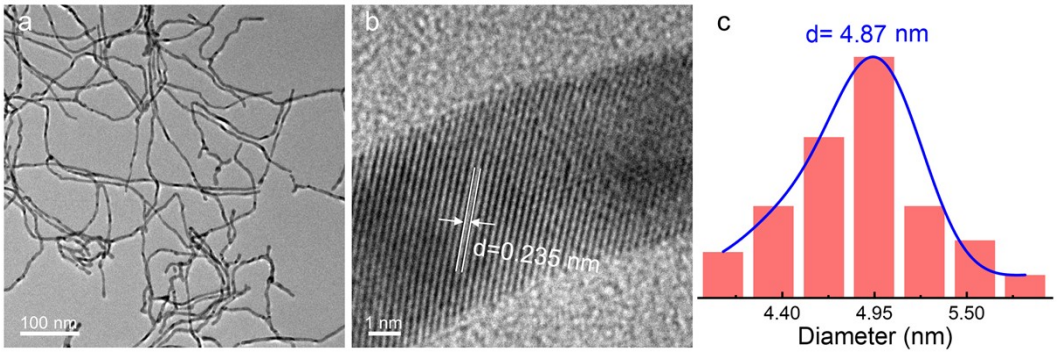

Fig. S1 (a) TEM image, (b) HRTEM image, and (c) particle-size distribution histogram of Au NWs.

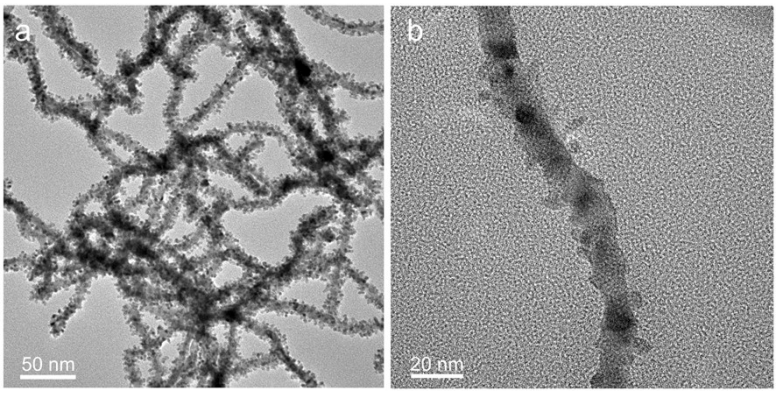

Fig. S2 TEM images of Au@PtPd@Pt NWs.

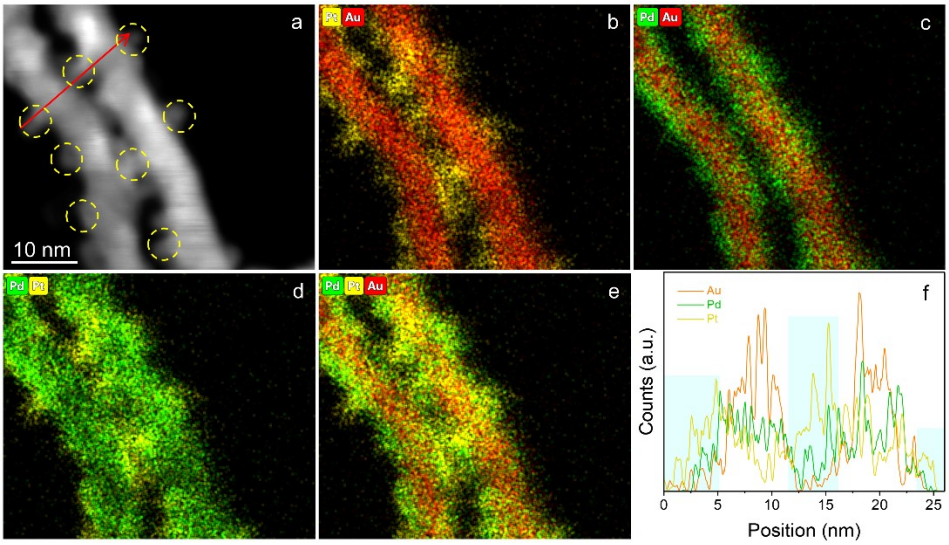

Fig. S3 Detailed characterizations of the core-shell-satellite structure in Au@PtPd@Pt NWs: (a-e) STEM image and the corresponding EDX elemental mapping images. (f) EDX line-scan profile.

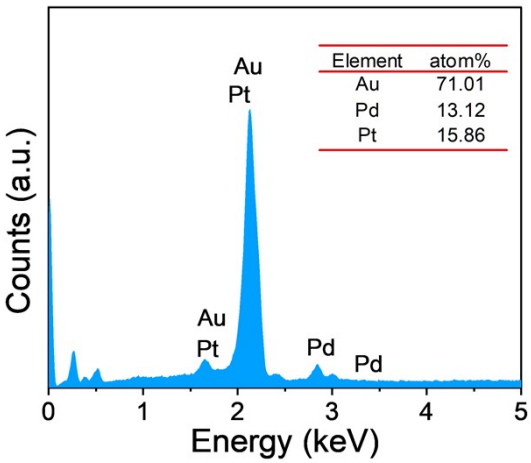

Fig. S4 EDX spectrum of Au@PtPd@Pt NWs.

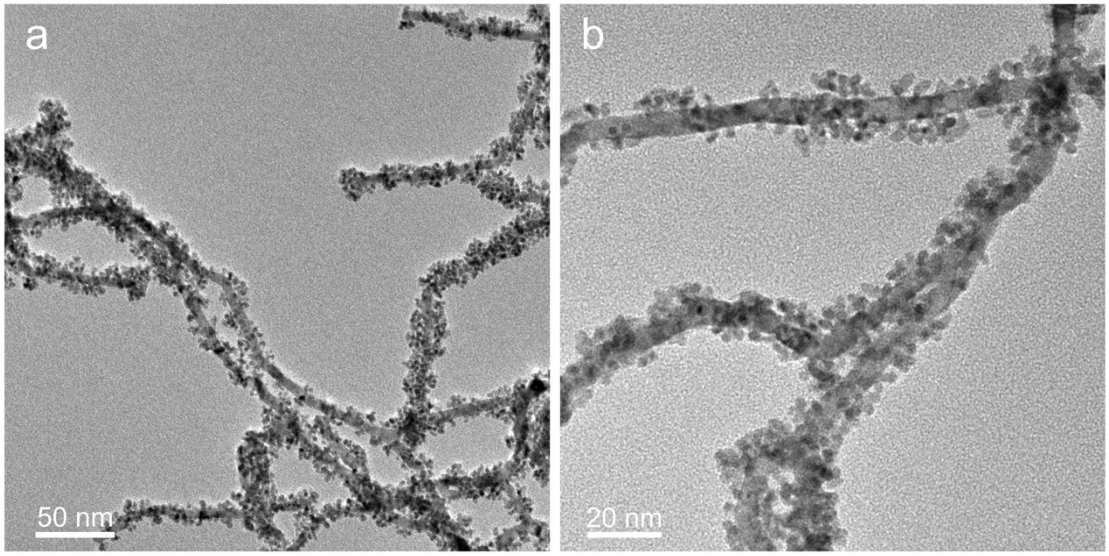

Fig. S5 TEM images of Au@Pt NWs.

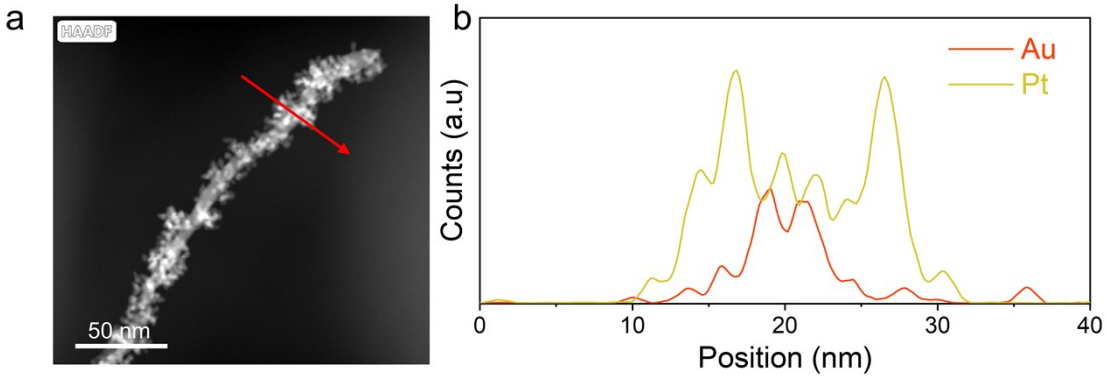

Fig. S6 STEM image and the corresponding EDX line-scan profile of Au@Pt NWs.

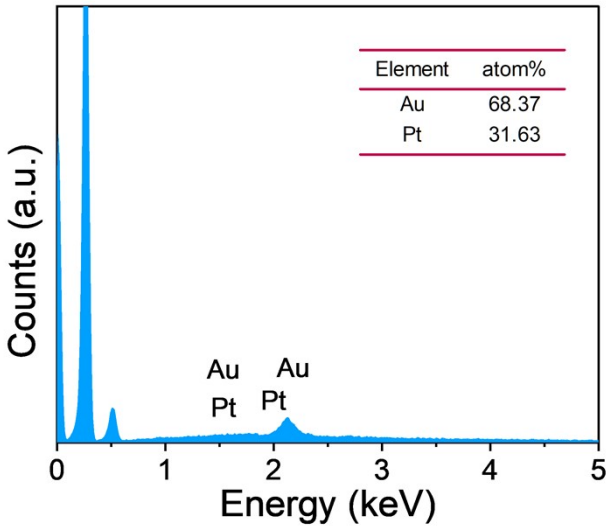

Fig. S7 EDX spectrum of Au@Pt NWs.

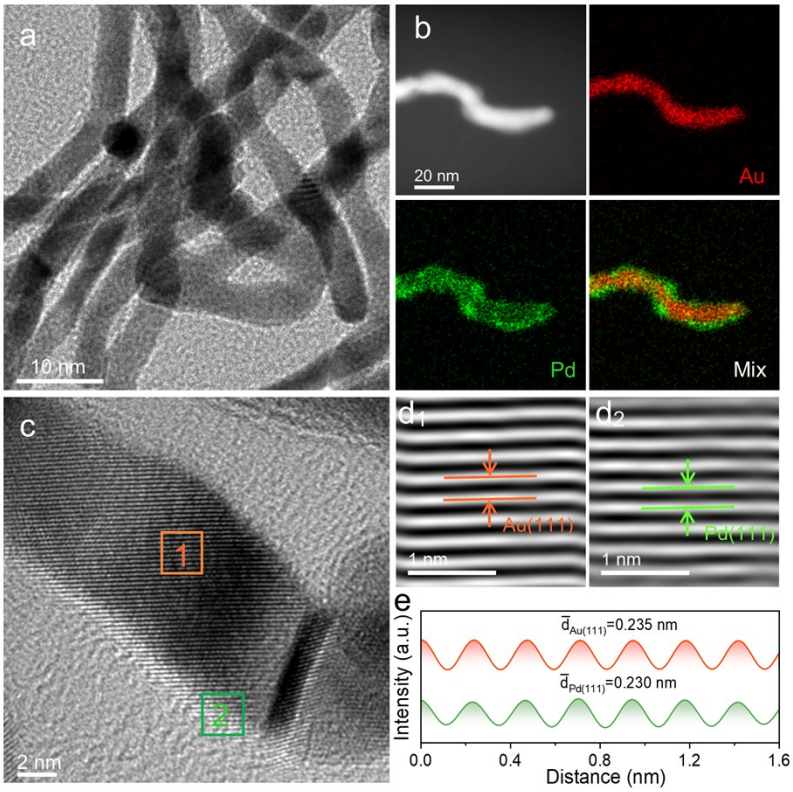

Fig. S8 Structural characterizations of Au@Pd NWs. (a) TEM image. (b) STEM image and the corresponding EDX elemental mapping images. (c) HRTEM image. (d) Fourier-filtered lattice fringe images taken from the rectangular regions in c, and (e) corresponding integrated pixel intensities.

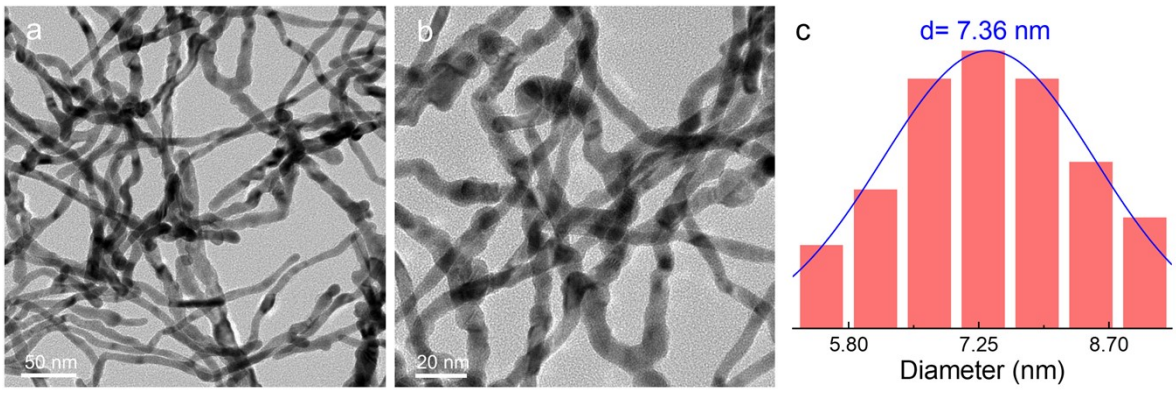

Fig. S9 (a-b) TEM images, (c) particle-size distribution histogram of Au@Pd NWs.

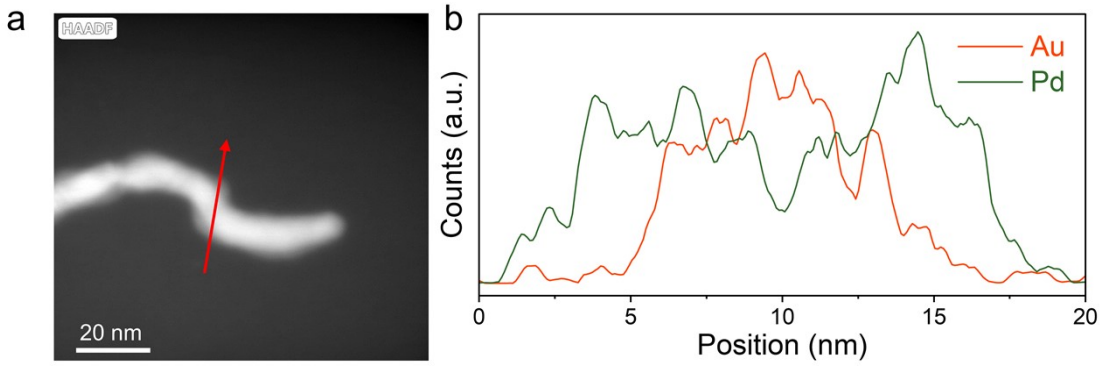

Fig. S10 EDX line-scan profile of Au@Pd NWs.

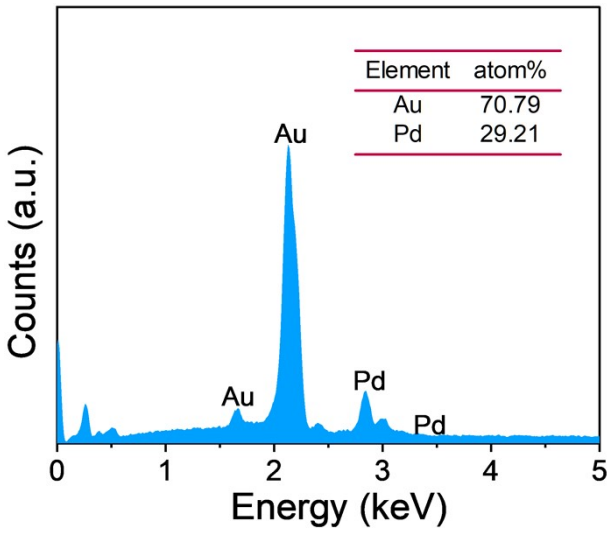

Fig. S11 EDX spectrum of Au@Pd NWs.

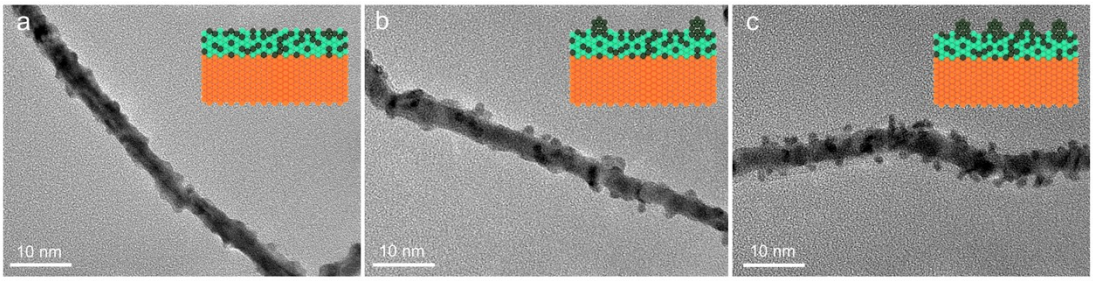

Fig. S12 TEM images of samples at different stages of the synthetic process of wire-like core-satellite Au@PtPd@Pt NWs: (a) 40, (b) 80, (c) 120 min.

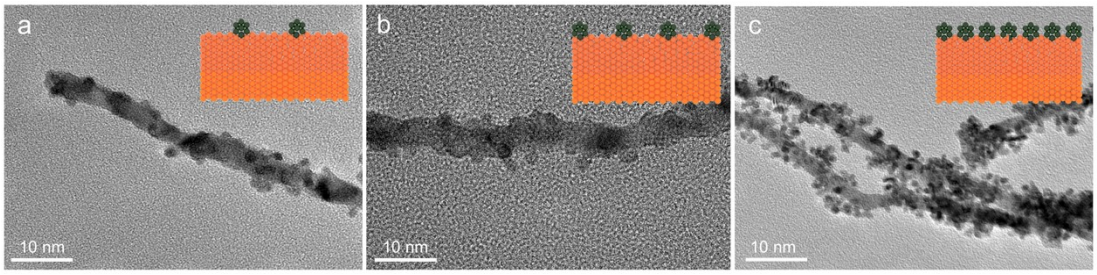

Fig. S13 TEM images of samples at different stages of the synthetic process of wire-like core-satellite Au@Pt NWs: (a) 40, (b) 80, (c) 120 min.

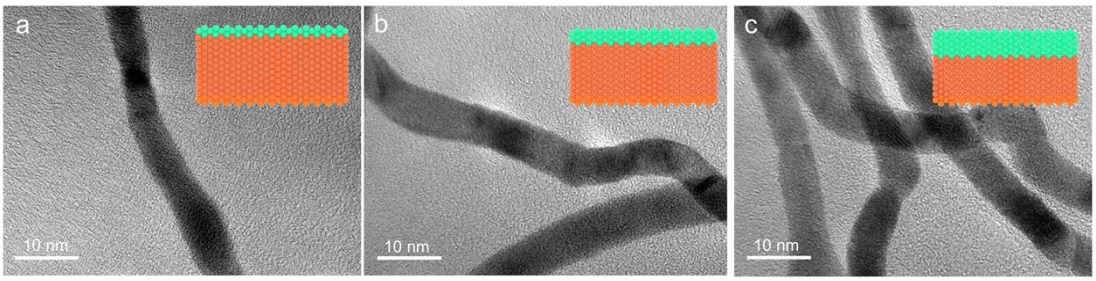

Fig. S14 TEM images of samples at different stages of the synthetic process of wire-like core-satellite Au@Pd NWs: (a) 40, (b) 80, (c) 120 min.

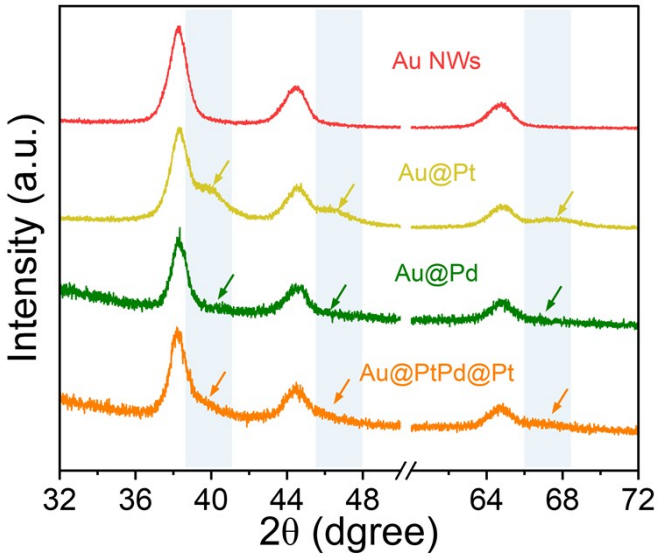

Fig. S15 Enlarged XRD patterns of Au, Au@Pd, Au@Pt and Au@PtPd@Pt NWs.

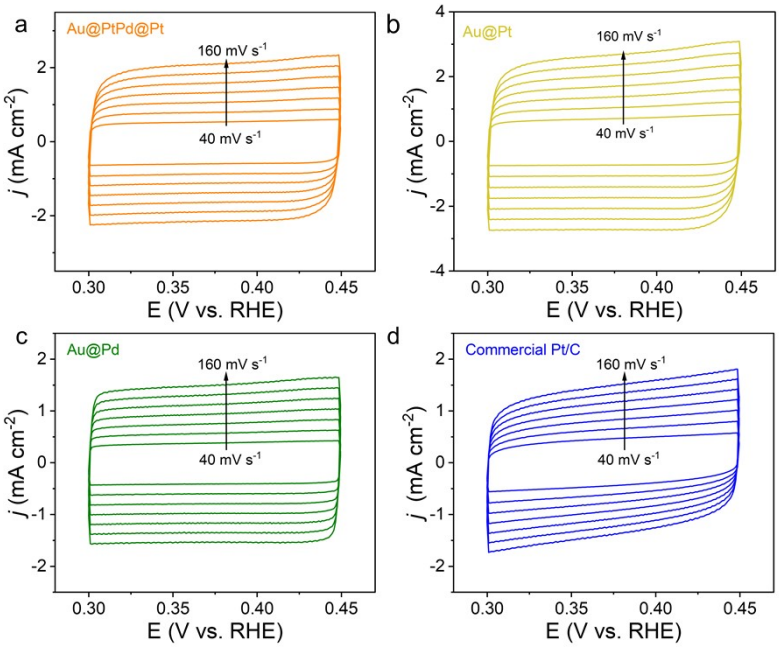

Fig. S16 CV plots of (a) Au@PtPd@Pt NWs, (b) Au@Pt NWs, (c) Au@Pd NWs, and (d) commercial Pt/C with varying scan rates from 40 to 160 mV s^{-1} in 1.0 M KOH.

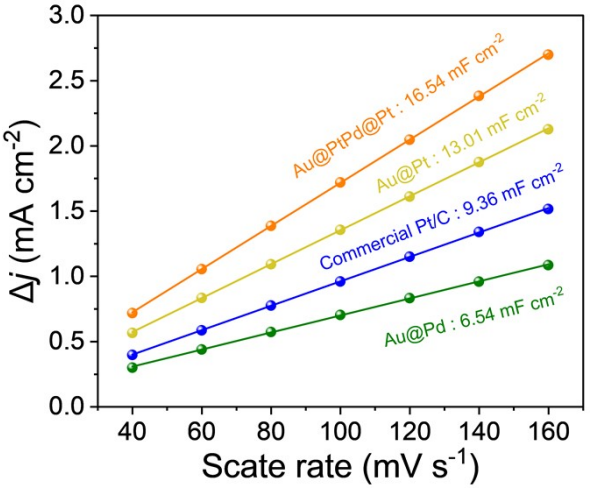

Fig. S17 The calculated C_{dl} values of the electrocatalysts.

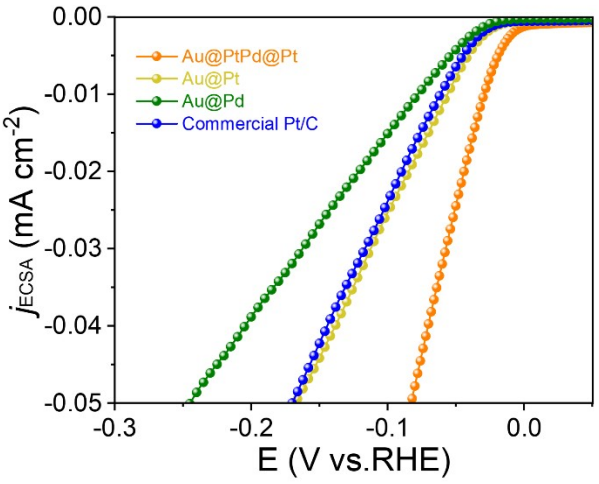

Fig. S18 The ECSA-normalized HER polarization curves of the catalysts in N_2-saturated 1.0 M KOH.

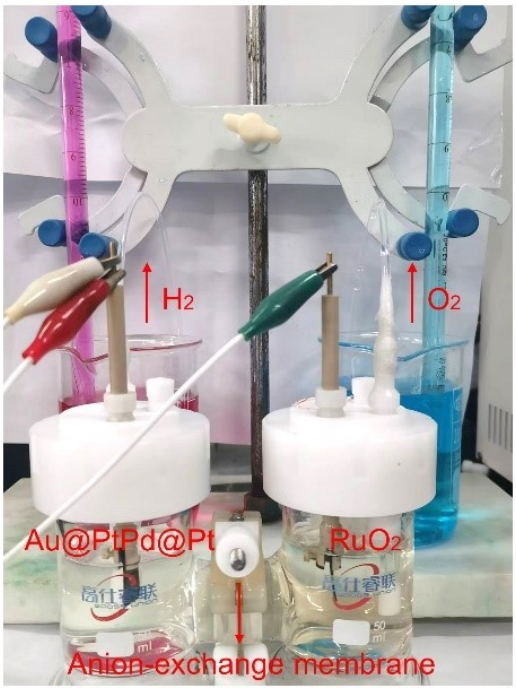

Fig. S19 Digital photograph of the water-splitting electrolyzer and corresponding gas-collecting device.

Table S1. The element content of the prepared catalysts obtained using ICP-OES and EDX.

Sample	ICP-OES Pt : Pd : Au (%)	EDX Pt : Pd : Au (%)
Au@PtPd@Pt	15.24 : 12.83 : 71.93	15.86 : 13.12 : 71.01
Au@Pt	29.98 : 0 : 70.02	31.63 : 0 : 68.37
Au@Pd	0 : 30.12 : 69.88	0 : 29.21 : 70.79

Table S2. Comparison of the HER activity with other reported noble and non-noble metal-based electrocatalysts in 1.0 M KOH.

Catalysts	η_{10} (mV)	Tafel Slope (mV dec^{-1})	Mass activity (A mg^{-1}@mV)	References
Au@PtPd@Pt	23	32	1.88 A mg^{-1}@50 mV	This work
Pt/Ni PCNFs	46	43.8	-	Chin. Chem. Lett. **2023**, 34, 107359
Pt/CuO NPC	39	41.7	-	Chem. Eng. J. **2023**, 455, 140856
PdPt bimetallenes	27.1	67.6	-	Carbon Energy **2023,** e367
Pt/TeO_x	33	29	-	Int. J. Hydrogen Energy **2023,** 48, 16593
Pt/$Ti_3C_2(OH)_x$	58	30	-	J. Mater. Chem. A **2023**, 11, 5328
Pd-CeO_2-x-NC	115	58	0.87 A mg_{Pt}^{-1}@50 mV	J. Colloid Interface Sci. **2022**, 611, 554
Pt@CoS	28	31	-	Appl. Catal. B: Environ. **2022**, 315, 121534
Pt/Pt_5P_2 nanocage	29	29.1	0.80 A mg_{Pt}^{-1}@100 mV	Adv. Funct. Mater. **2022**, 32, 2205985
Pt/NiO flowers	66	82	0.91 A mg_{Pt}^{-1}@66 mV	Int. J. Hydrogen Energy. **2022**, 47, 33988
Ru-Te nanorods	37	61.6		Nanoscale **2022**, 14, 14913
Pd_1-$CoSe_2$ NBs	42	78	-	Appl. Catal. B: Environ. **2021**, 295, 120280
Pd-e-NiCo-PBA-C	147	67	-	Adv. Funct. Mater. **2021**, 31, 2008989.
NiPd alloy	38	168	-	Chem. Eng. J. **2021**, 411, 128486
$PtSe_2$/Pt	42	53	-	Angew. Chem. Int. Ed. **2021**, 60, 23388
$PtSe_2$ nanosheet	138	100	-	Adv. Funct. Mater. **2021**, 31, 2102321
Pt/$Ni(OH)_2$/NF	25.9	37.6	0.81 A mg_{Pt}^{-1}@50 mV	Int. J. Hydrogen Energy **2020**, 45, 27067
Pt/NiO/Ni/CNT	217	90.1	0.30 A mg_{Pt}^{-1}@50 mV	Nanoscale **2020**, 12, 14615
FeCoNiRu-450	40	84	1.31 A mg^{-1}@100 mV	Adv. Sci. **2023**,10, 2300094
NiO@1T-MoS_2	46	52	-	Nat. Commun. **2019**, 10, 982
Co_3S_4 PNS_{vac}	63	58	1.06 A mg^{-1}@200 mV	ACS Catal. **2018**, 8, 8077-8083
NiO/PtNi	40	79	-	J. Am. Chem. Soc. **2018**, 140, 8982
Ni_3S_2/NF	240	152	-	Adv. Energy Mater. **2018**, 8, 1703538
NiCoN/C	103	--	2.04 A mg^{-1}@200 mV	Adv. Mater. **2019**, 31, 1805541
Ni-Mo-N	40	70	-	Nat. Commun. **2019**, 10, 5335
Ni-BDT-A	80	70	-	Chem **2017**, 3, 122
CoP UPNSs	56	44	0.15 A mg^{-1}@100 mV	Chem. Sci., **2017**, 8, 2769-2775
CuNi NC	140	79	-	ACS Catal. **2019**, 9, 5084

References

1 X. Jiang, X. Qiu, G. Fu, J. Sun, Z. Huang, D. Sun, L. Xu, J. Zhou and Y. Tang, Highly simple and rapid synthesis of ultrathin gold nanowires with (111)-dominant facets and enhanced electrocatalytic properties, *J. Mater. Chem. A*, 2018, **6**, 17682-17687.

2 Y. Y. Liang, Y. G. Li, H. L. Wang, J. G. Zhou, J. Wang, T. Regier and H. J. Dai, Co_3O_4 nanocrystals on graphene as a synergistic catalyst for oxygen reduction reaction, *Nat. Mater.*, 2011, **10**, 780-786.